Presented at the 20th Conference on Integrated Observing and Assimilation Systems
for the Atmosphere, Oceans and Land Surface (IAOS-AOLS),
New Orleans, LA, January 11-14, 2016,
Amer. Meteor. Soc., Paper 10.6

10.6 TUNING AN ANALYSIS AND INCREMENTAL ANALYSIS UPDATING ASSIMILATION FOR AN EFFICIENT HIGH-RESOLUTION FORECAST SYSTEM

Keith A. Brewster*[1] and Derek R. Stratman[2]

[1]Center for Analysis and Prediction of Storms
[2]School of Meteorology
University of Oklahoma
Norman, OK 73072

1. INTRODUCTION

The Dallas/Ft. Worth Urban Testbed (D/FW Testbed) has been established as a site for evaluating real-time observing systems, data analysis and short-term forecasting over an urban area. A number of high-density observing networks are being tested in the region, including X-band Doppler radars, citizen weather observations, mobile sensors, and ground based profilers. These systems along with the Federal surface and radar networks comprise the diverse data that the Center for Analysis and Prediction of Storms (CAPS) is utilizing in our real-time analysis, nowcasting and short-term numerical weather prediction (NWP) efforts.

Building on our experience with the Collaborative-Adaptive Sensing of the Atmosphere (CASA) Integrated Project-1 (IP1) in Oklahoma (McLaughlin et al. 2009) we have configured a 3DVAR with cloud analysis system with 400-m grid spacing and an efficient Numerical Weather Prediction (NWP) system with 1-km grid spacing for 0-to-2 hour forecasts with low latency. Besides providing real-time information for local governments and the National Weather Service (NWS) Forecast Office in Fort Worth, the system can be used as a basis for the testing of observation system impacts, including Networks of Networks (NRC, 2009) that are being integrated into the National Mesonet Program. Some of that work is described in Carr et al, 2016.

This paper describes tests of the recently-developed Incremental Analysis Updating with Variable-Dependent Timing (IAU-VDT) assimilation method that is now being used in the real-time forecasts. The IAU-VDT allows the timing of the introduction of analysis increments to differ for each variable. Real time analysis and forecasting products from the 26 Dec 2015 tornadoes in the D/FW metro area are presented as sample results.

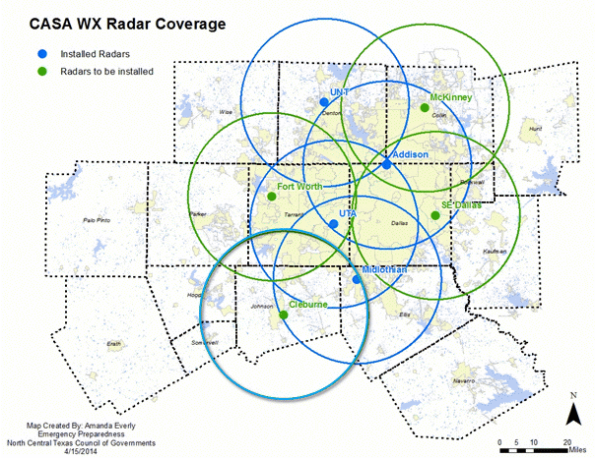

Figure 1 Current status of CASA X-band Radar Network in the D/FW Testbed. Blue circles indicate 40-km range rings for radars currently deployed. Green circles are for planned radar sites, expected to be deployed in 2016. Background map shows county boundaries of the NCTCOG

2. CASA DALLAS-FORT WORTH TESTBED

Beginning in 2012 some of the CASA IP-1 X-band radars were moved to North Texas from Oklahoma to be the cornerstone of the newly-established D/FW Urban Testbed with the support of the North Central Texas Council of Governments (NCTCOG), the NWS and other public and private sector partners.

As of January, 2016 there are five X-band radars deployed in the CASA D/FW Testbed (Fig 1), two relocated from the original CASA IP1 Network in southwestern Oklahoma, and one each from Ridgeline Instruments, EWR, Furuno, and Enterprise Electronics (EEC). Another IP1 radar

*Corresponding author address: Keith Brewster,
120 David L. Boren Blvd., Suite 2500,
Norman, OK 73072, kbrewster@ou.edu

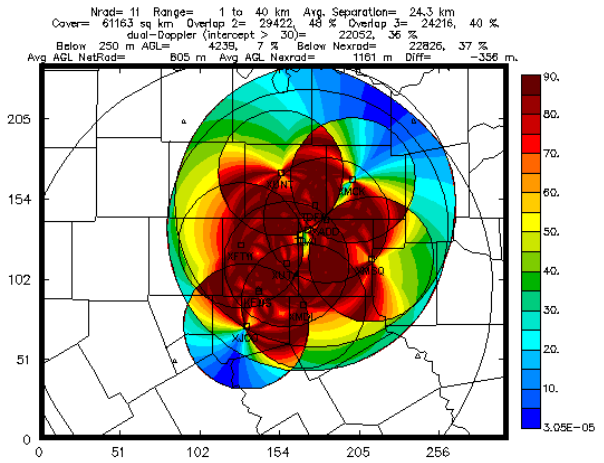

Figure 2. Maximum dual-Doppler crossing angles (color, degrees, scale at right) for combined CASA X-band (40 km range rings), TDWR and NEXRAD radar network.

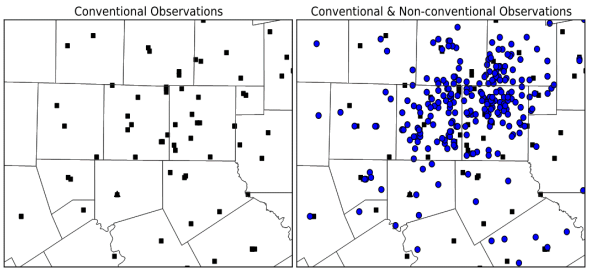

Figure 3. Sample station location plot for surface stations in the D/FW Testbed area from 15 May 2013. Left: Conventional AWOS and ASOS sites. Right; non-conventional stations including CWOP and EarthNetworks WxBug sites

has recently been hoisted onto a tower in northwest Ft. Worth and should be online soon. Two other sites, at Mesquite and McKinney, are in planning stages. These radars are in addition to the three Federal radars in the metro area, namely the NEXRAD (WSR-88D) at Fort Worth (KFWS) and Federal Aviation Administration (FAA) Terminal Doppler Weather Radar (TDWR) serving Dallas Love Field (TDAL) and the TDWR serving the Dallas/Ft Worth Airport (TDFW). The analysis and forecast system also utilize other, more distant, NEXRAD radars that cover portions of their domains.

The combined Doppler radar network has good to excellent dual-Doppler crossing angles (Fig 2) and low-level coverage over the NCTCOG region and especially over the densely populated Dallas and Tarrant Counties.

In addition to the radars and conventional surface observation systems, a number of additional non-conventional instruments are in the region, or will soon be brought into the testbed, as listed in Table 1. To highlight a few, the standard suite of surface observations from the NWS and FAA are augmented with additional surface observations from the EarthNetworks WeatherBug network as well as the NOAA Citizen Weather Observer Program (CWOP), e.g. Fig 3. Additionally, mobile data from commercial trucks are provided by the Mobile Platform Environmental Data (MoPED) system from GST, Inc. (Heppner, 2013). SODARs from WeatherFlow, Inc., and temporary deployments of low-level profiling units from the NSSL/OU Collaborative Lower Atmospheric Mobile Profiling System (CLAMPS) have also been used. Just recently TAMDAR (Tropospheric Airborne Meteorological Data Reporting) profiles from the regional commercial airliners have also been added to the data available and will soon be added to our processing workflow.

Table 1. Observations in Dallas-Ft Worth Testbed

Conventional Observations	Non-Conventional Observations
ASOS	EarthNetworks (WxBug)
AWOS	CWOP
	GST MoPED
	Oklahoma & West Texas Mesonets
S-band WSR-88D	X-band Radars
	C-band TDWR Radars
Radiosondes	SODAR
	Radiometers

3. REAL-TIME ANALYSES AND FORECASTS DESIGN

CAPS designed a 400-m grid resolution real-time analysis and 1-km real-time data assimilation, nowcasting and NWP system using the Advanced Regional Prediction System (ARPS, Xue et al., 2001; Xue et al., 2003), and the ARPS 3D-Variational (3DVAR) with cloud analysis (Gao et al., 2004; Brewster et al., 2005; Hu et al. 2006a,b,

Brewster et al., 2015) and ran the system in a domain covering central and southwest Oklahoma (Brewster et al., 2007 and 2010). The system as repositioned for the D/FW Testbed is described below with summary details for the analysis and forecast in Tables 2 and 3, respectively.

The analysis is performed every 5 minutes on a 160x160 km grid with 400 m resolution. The focus for the analysis on tracking low-level signatures of storms and precursors for convective initiation so the top of the analysis domain is 15 km AGL, using 28 vertical levels with an average spacing of 600 m, and minimum of 20 m near the ground, first level at anemometer height (10 m AGL). The analyses are run on 192 Intel Xeon Sandy Bridge cores of Boomer at the OU Supercomputing Center for Research and Education (OSCER). The total time for the analyses, including image post processing is about 6 minutes so two sets of cores are used.

Data assimilation and short-term forecasting are run on a 350 x 320 km domain with 1-km grid spacing. 53 vertical grid levels are used with domain top at 20 km and enhanced vertical resolution near the ground (20 m minimum vertical grid spacing). The assimilation process, including recent upgrade and tuning are described in Section 4.

Table 2. Features of Real-Time 400-m Analyses

Method	3DVAR & Complex Cloud Analysis
Processors	192 Cores MPI
Interval	5 minutes
Typical Run Time	~6 minutes
Grid Spacing	400 m
Vertical Grid Spacing	600 m mean 20 m minimum
Grid Dimensions	448 x 456 x 28

Table 3 Features of Real-Time NWP Forecasts

Model	ARPS
Assimilation	2 cycles IAU
Processors	192 Cores MPI
Interval	15-30 minutes
Forecast Time	0-2 hours
Typical Run Time	20-25 minutes
Grid Spacing	1 km
Vertical Grid Spacing	400 m mean 20 m minimum
Grid Dimensions	363 x 323 x 53

For the short-term forecast there is no cumulus parameterization, clouds and precipitation are modeled using the Lin 3-Ice scheme (Lin et al., 1983). The model uses NASA Goddard atmospheric radiation transfer parameterization. Surface fluxes are calculated from stability-dependent surface drag coefficients using predicted surface temperature and volumetric water content. The model employs 1.5-order TKE closure based on Sun and Chang (1986), and a simple two-layer force-store soil model based on Noilhan and Planton (1989).

The NWP model is run when there is significant precipitation in the D/FW Testbed area or when precipitation is expected and the X-band radars are running. The model is run on 192 cores of OSCER Boomer every 15-30 minutes. The model, including image post-processing takes about 20-25 minutes to run so two sets of cores are used.

Interested readers can find the real-time analysis and forecast products on the Web during our operational periods via the links at http://forecast.caps.ou.edu .

4. IAU WITH VARIABLE-DEPENDENT TIMING

Data are assimilated in the forecast system by calculating the increments from the most recent 12-km NAM background forecast valid at the 10-minutes before the nominal initial time using 3DVAR, then applying the analysis increments in an incremental analysis updating scheme (IAU, Bloom et al., 1996) over a 10 minute data window. Then, a 2-hour forecast is run, including a second IAU cycle. The IAU allows the model to ingest the observation information, including the cloud and precipitation variables and associated latent heating, while allowing the model to come into balance by the end of the assimilation window.

Traditionally the IAU assimilation is applied with a triangular distribution of the fractional increments in time such that the largest fraction of the increment is applied in the middle of the time window, ramping up from zero at the beginning and then back down to smoothly transition to zero

fractional increment being applied by the end of the window. The increments were applied using the same distribution in time for all variables. Examining the vertical cross sections in cases of strong thunderstorms and/or squall lines in the initial conditions revealed some difficulties in establishing an updraft in a strong convective storm from a larger-scale background without such a storm. There was some evidence in the first IAU cycle of difficulty in maintaining the observed hail/graupel maxima.

From this experience a hypothesis emerged: Support of the weight of the hail, graupel and heavy rain would be improved by first adjusting the wind and mass fields to allow the updraft velocities to become established without significant rain and hail loading and/or decelerating cooling due to melting of hail and/or graupel. This can be accomplished by adjusting the increment distribution in time so that a larger fraction of the latent heat and wind increments are applied early in the IAU window, and also introducing the hydrometeors using a different time weighting that applies most of those increments toward the end of the IAU window. This feature was added to our assimilation software and named, IAU with Variable-Dependent Timing (IAU-VDT).

The ARPS IAU code was modified to allow user specification of the IAU increment distribution in time by specifying one or more shapes and then assigning a shape to each variable. To test the IAU-VDT, we define three shape couples, the centered triangular shape uniformly applied to all variables as is commonly used in IAU systems (Shape A, Fig 4a), a triangular weighting that is biased toward the beginning of the assimilation window to be used for temperature, water vapor and wind fields with a triangular weighting biased toward the end of the assimilation window to be applied to hydrometeor increments (Shape B, Fig. 4b), and a weighting for temperature, water vapor and wind as in Shape B, but with the start of hydrometeor insertion delayed until the middle of the assimilation window (Shape C, Fig. 4c).

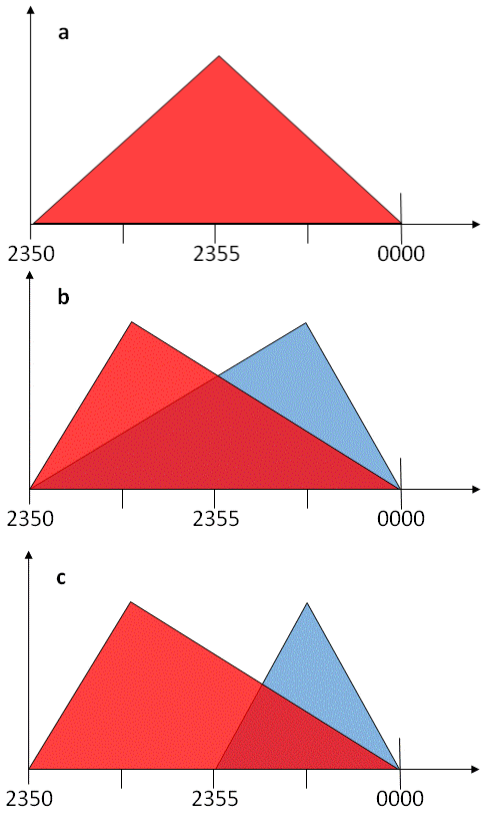

Figure 4 Three IAU-VDT time weighting shape pairs: a) A: Uniform triangular weighting b) B: early mass-wind bias (red) with late hydrometeor bias (blue) c) C: early mass-wind bias (red) with delayed-start hydrometeor insertion (blue)

The test case will be 24 April 2015, a day featuring a strong squall line passing through the CASA D/FW Testbed with wind high winds and hail observed (Fig 5). We will examine east-west vertical cross-sections as along y=40.5 km as indicated by horizontal line in Fig 5.

Figure 6 shows the hydrometeor estimates from the cloud analysis using the Milbrant and Yau single-moment microphysics (Milbrant and Yau, 2005a, 2005b). A hail and graupel core is analyzed with maxima as indicated in the first column of Table 4.

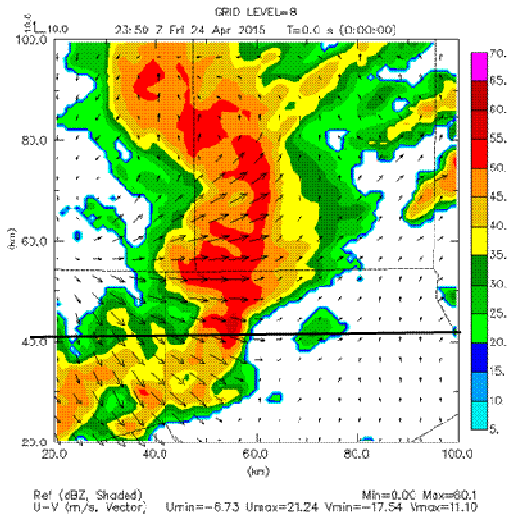

Figure 5 Initial reflectivity (dBZ, colors) and wind at grid level 8 at 2350 UTC (using mosaicked data from 2350-UTC) that is used to generate analysis increments for IAU in the 2350-0000 assimilation window. Cross-sections along y=40.5 km as indicated by horizontal line.

Figure 7 shows the result of the 10-minute forecast/assimilation with the analysis increments applied using the three IAU-VDT time weighting schema previously described. The maxima after the assimilation are recorded in columns 3-5 of Table 4. Comparing the three panels in Fig. 7 it is apparent that there is improvement in retention of updraft vertical velocity, hail and graupel using Scheme B over the traditional equally-weighted Scheme A, particularly in the hail core between 3 and 6 km. There is additional improvement when delaying the start of hydrometeor assimilation as shown in the results for Scheme C, again in the hail core aloft as well as in the maximum values of graupel and hail. It is also evident that there is improvement in the structure of the hail core, being less spread out horizontally in the lowest 3 km, after applying Scheme C compared to the other IAU time weighting shapes.

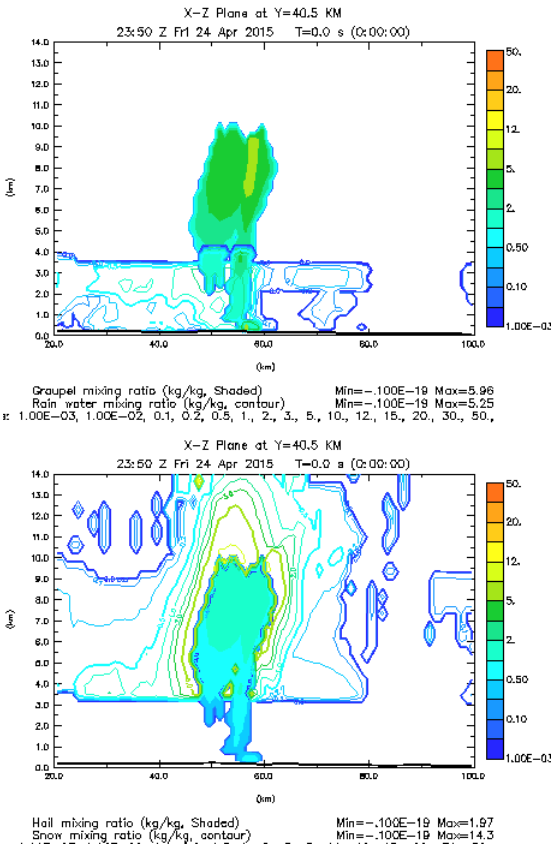

Figure 6 East-west cross-section at y=40.5 km. Estimated hydrometeor fields from the complex cloud analysis at 2350 UT. Top panel: graupel (color) and rain (colored contour lines). Bottom panel: hail (color shading) and snow (color contours).

Table 4 Maxima of Selected Variables at End of IAU time window (2350-0000 UTC)

Variable	Analysis	IAU-Orig	IAU-B	IAU-C
Rain	5.3 g/kg	2.4	2.7	3.3
Snow	14.3 g/kg	4.0	5.3	10.0
Graupel	6.0 g/kg	2.1	2.1	2.0
Hail	2.0 g/kg	0.3	0.3	0.6
W	8.4 m/s	6.2	7.5	7.9

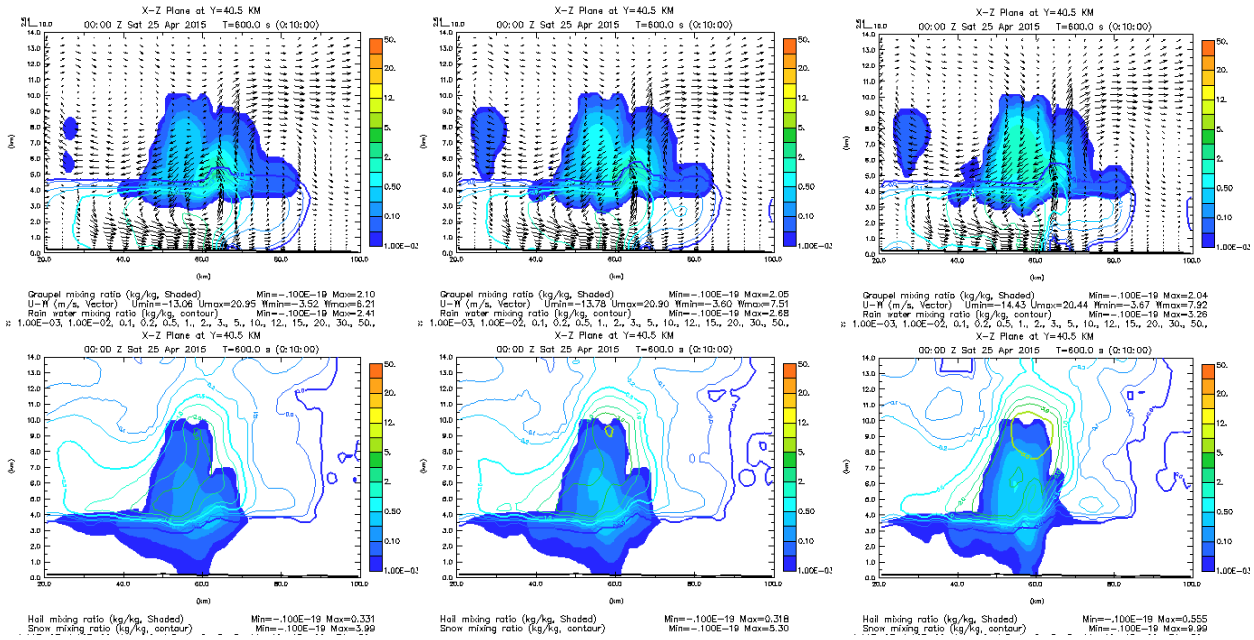

Figure 7. Cross-section at y=40.5 km after 10-min IAU assimilation window. Variables as in Fig 12. Left IAU-VDT time weighting scheme A, Center: IAU-VDT scheme B, Right: IAU-VDT scheme C.

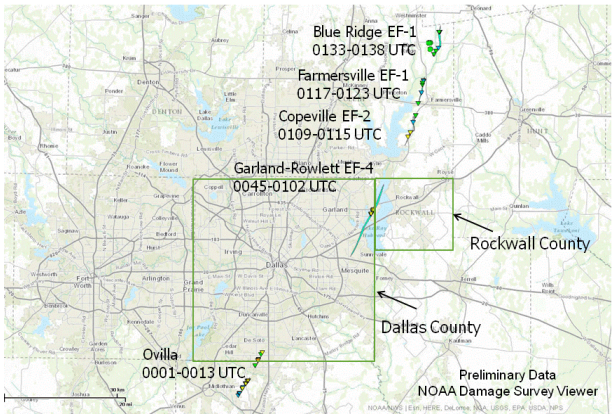

Figure 8. Tornado tracks near Dallas on 26-Dec-2015 (UTC Times 27-Dec-2015). Dallas and Rockwall Co. are highlighted to aide reader orientation with model output figures. From NOAA Damage Survey Viewer.

5. GARLAND-ROWLETT, TX TORNADO CASE

Example products from the analysis system and newly-updated assimilation and forecast system are presented from a recent significant event in the Dallas-Ft. Worth region.

In the late afternoon and early evening of 26 December 2015 supercell thunderstorms moved generally north-northeast across the Dallas Metroplex. Among the tornadoes in the Dallas area were an EF3 tornado near Ovilla around 00 UTC 27 Dec and 45 minutes later a large long-track tornado (approximately 20 km long, 500 m wide) with EF4 damage rating that touched down just south of Interstate-30 in Sunnyvale and passed through the portions of Garland and Rowlett in the northeast part of the metro area (Fig. 8). Following that, there were additional tornadoes to the north-northeast of Rowlett as the parent storm continued tracking in that direction.

The analyses around the time of the Ovilla tornado are shown in Fig. 10 for the period 0000 to 0015 UTC. The 3DVAR identifies the parent circulation center in the wind and vorticity plots. Though there is some smoothing inherent in the process, this analysis makes identification easier for those not familiar with interpreting the raw Doppler radar radial velocities. Based on these plots, some additional tuning of the 3DVAR may be done to better preserve the wind maxima near such features.

It is of interest to note the cycling of the rotation that is occurring as the western circulation center

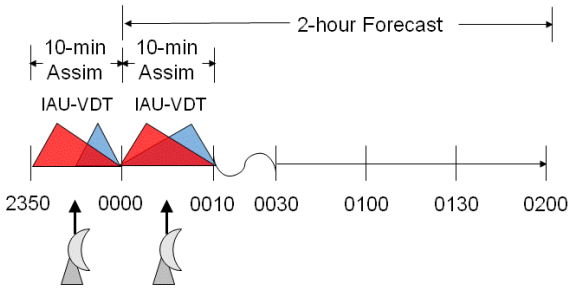

Figure 9. Data assimilation timeline diagram for a sample 0000 UTC forecast initial time, showing observation insertion in two IAU-VDT steps as part of a 2-hour forecast

wraps-up the reflectivity field, there is a new circulation center beginning to form on the southeast gradient of the reflectivity. Also note the more compact storm entering the analysis domain from the south that also has rotation indicated in the winds and vorticity and also suggested in the reflectivity structure.

The real-time NWP system had been updated with the new IAU-VDT assimilation scheme, and used as indicated in Fig 9. Two analysis and assimilation cycles are performed. In the first, Scheme C in Fig. 4 is utilized. For the second cycle, the assumption is the updraft will have been established so the more moderate timing offset of Scheme B in Fig. 4 is applied.

The forecast system on this day was being run at 30 minute intervals. The forecasts were very successful in maintaining the storms and producing very strong rotation as indicated in the 1-6 km updraft helicity (UH) plots. Figure 11 shows four successive real-time forecasts (initialized 2300 to 0030) at the valid time for each where the forecast was indicating a strong UH field near the starting point of the Garland-Rowlett tornado. The tornado damage survey points are show as the triangles in the plot, the contours are reflectivity in 10 dBZ intervals with the UH indicated in color contours, non-linear scale at right. The timing of the rotation center was a bit fast in each, with successive forecasts asymptotically approaching the 0045 actual estimated time of touchdown. The forecast initialized at 2330 UTC was the strongest at the time of touchdown and also through most of the track. Based on this and other cases there seems to be about a 15-20 minute spin-up time for the model to develop full strength of circulations and updrafts, thus the forecast initialized at 0000 UTC is actually the weakest at the time of touchdown.

Fig 11 shows a sequence of forecast images from the forecast initialized at 2330 UTC. The

sequence shows forecasts out 50 min to 1:30 into the forecast. Given that the latency for the 2-hour output is about 20-25 minutes these forecasts had nearly one hour actual lead time on the observed 0045 UTC touch down time. The forecasts were quite accurate on the location of the maximum UH which were nearly coincident with the actual track. The UH values were extremely strong, peaking at more than 3000 m^2s^{-2}.

Overall the forecasts performed remarkably well for this grid scale and showed good run-to-run consistency in the development and locations of the strongest rotation.

6. SUMMARY AND FUTURE WORK

A real-time high-resolution data analysis and short-term NWP system has been set-up for the D/FW Testbed. A unique enhancement to the IAU assimilation scheme has been developed and tested, IAU with Variable-Dependent Timing (IAU-VDT). This method, as demonstrated with the 26-Dec-2015 case, has been implemented in our real-time workflow and is producing quality short-term forecasts. Use of a one- or two-moment Milbrandt and Yau scheme is planned for the real-time system after an OSCER computer upgrade is completed – anticipated by March, 2016.

At the time of publication five X-band radars have been sited, and locations for additional X-band radars have been identified considering needs for dual-Doppler analysis, low-level coverage and deployment logistics. We expect at least six X-band radars will be operational in Spring 2016.

Beginning in Spring 2016, formal quantitative evaluation will be done of precipitation forecasts using Equitable Threat Scores and object-based methods for tornadoes, following recent work of Stratman and Brewster (2015). Separately, training of forecasters and emergency managers in the use of these and other CASA tools will also be done in the coming year, with subjective evaluation by other stakeholders to follow, based on results.

One objective of the D/FW Testbed, as part of the National Mesonet effort, is to identify the impact of the novel observation systems on the analyses and forecasts. This will be carried-out via OSEs, OSSEs and evaluation of analysis sensitivity to each data source. Some preliminary work in this area is described in Carr et al., 2016.

7. ACKNOWLEDGMENTS

The D/FW Testbed and CASA work is supported in part by the National Science Foundation (NSF) under EEC03-13747, by the National Weather Service Mesonet Program, and the North Central Texas Council of Governments. Brenda Philips and Apoorva Bajaj of the University of Massachusetts lead the D/FW CASA X-band Testbed activities.

The authors would like to thank ROC staff, particularly Tim Crum, and Karen Cooper of NSSL for their help in gaining access to the real-time Level-II FAA TDWR data for the D/FW Testbed. Thanks to all private partners who provided real-time radar and other data.

Oklahoma Mesonet data provided by the Oklahoma Climatological Survey. West Texas Mesonet data provided by Texas Tech University.

Supercomputing resources from the Oklahoma University Supercomputer Center for Education and Research (OSCER) were used for the analyses and forecasts in this study.

Any opinions, findings, conclusions, or recommendations expressed in this material are those of the authors and do not necessarily reflect those of the funding agencies nor the host universities.

8. REFERENCES

Bloom, S. C., L. L. Takacs, A. M. da Silva, D. Ledvina, 1996: Data Assimilation Using Incremental Analysis Updates. *Mon. Wea. Rev.*, **124**, 1256–1271.

Brewster, K.A. F.H. Carr, K.W. Thomas and D.R. Stratman, 2015: Utilizing heterogeneous radar systems in a real-time high resolution analysis and short-term forecast system in the Dallas/Ft. Worth Testbed. *Preprints, 37th Conference on Radar Meteorology*, Amer. Meteor. Soc., Paper 31.

Brewster, K., M. Hu, M. Xue, and J. Gao, 2005: Efficient assimilation of radar data at high resolution for short range numerical weather prediction. World Weather Research Program Symposium and Nowcasting and Very Short-Range Forecasting WSN05, Toulouse, France. WMO World Weather Research Program, Geneva, Switzerland. Symposium CD, Paper 3.06.

Brewster, K.A. and D.R. Stratman, 2015: An updated high-resolution hydrometeor analysis system using radar and other data. *Preprints, 27th Conference on Wea. Analysis and Forecasting and 23rd Conf. on Numerical. Wea. Pred.*, Amer. Meteor. Soc., Paper 31.

Brewster, K.A., K. W. Thomas, J. Brotzge, Y. Wang, D. Weber, and M. Xue, 2007: High resolution

assimilation of CASA X-band and NEXRAD radar data for thunderstorm forecasting. 22nd Conf. Wea. Anal. Forecasting/18th Conf. Num. Wea. Pred., Salt Lake City, Utah, Amer. Meteor. Soc., Paper 1B.1

Brewster, K., K.W. Thomas, J. Gao, J. Brotzge, M. Xue, and Y. Wang, 2010: A nowcasting system using full physics numerical weather prediction initialized with CASA and NEXRAD radar data. Preprints, 25th Conf. Severe Local Storms, Denver, CO, Amer. Meteor. Soc., Denver, CO, Paper 9.4.

Carr, F., M. Morris, A. Osborne, and K.A. Brewster, 2016: 20th Conference on Integrated Observing and Assimilation Systems for the Atmosphere, Oceans and Land Surface (IAOS-AOLS), 85th Amer. Meteor. Soc. Annual Meeting CD, Paper: P3.4

Gao, J., M. Xue, K. Brewster, and K. K. Droegemeier 2004: A three-dimensional variational data assimilation method with recursive filter for single-Doppler radar, *J. Atmos. Oceanic. Technol.* 457-469.

Heppner, P.O.G, 2013, Building a National Network of Mobile Platforms for Weather Detection, 29th Conf. on Environ. Information Processing Technologies, Amer. Meteor. Soc., Recorded presentation: https://ams.confex.com/ams/93Annual/recordingredirect.cgi/id/23230

Hu, M., M. Xue, and K. Brewster, 2006a: 3DVAR and cloud analysis with WSR-88D Level-II Data for the Prediction of Fort Worth Tornadic Thunderstorms Part I: Cloud analysis and its impact. *Mon. Wea. Rev.*, **134**, 675-698.

Hu, M., M. Xue, J. Gao and K. Brewster: 2006b: 3DVAR and Cloud Analysis with WSR-88D Level-II Data for the Prediction of Fort Worth Tornadic Thunderstorms Part II: Impact of radial velocity analysis via 3DVAR, *Mon Wea Rev.*, **134**, 699-721.

Lin, Y.-L., R. D. Farley, and H. D. Orville, 1983: Bulk Parameterization of the Snow Field in a Cloud Model. *J. Climate Appl. Meteor.*, 22, 1065–1092.

McLaughlin, D. D. Pepyne, V. Chandrasekar, B. Philips, J. Kurose, M. Zink, K. Droegemeier, S. Cruz-Pol, F. Junyent, J. Brotzge, D. Westbrook, N. Bharadwaj, Y. Wang, E. Lyons, K. Hondl, Y. Liu, E. Knapp, M. Xue, A. Hopf, K. Kloesel, A. Defonzo, P. Kollias, K. Brewster, R. Contreras, B. Dolan, T. Djaferis, E. Insanic, S. Frasier, and F. Carr, 2009: Short-Wavelength Technology and the Potential For Distributed Networks of Small Radar Systems. *Bull. Amer. Meteor. Soc.*, 90, 1797-1817.

Milbrandt, J. A. and M. K. Yau, 2005a: A Multimoment Bulk Microphysics Parameterization. Part I: Analysis of the Role of the Spectral Shape Parameter. *J. Atmos. Sci.*, 62, 3051–3064.

Milbrandt, J. A. and M. K. Yau, 2005b: A Multimoment Bulk Microphysics Parameterization. Part II: A Proposed Three-Moment Closure and Scheme Description. *J. Atmos. Sci.*, 62, 3065–3081.

National Research Council, 2009, *Observing Weather and Climate from the Ground Up. A Nationwide Network of Networks.* The National Academies Press, Wash. DC, 250 pp. http://books.nap.edu/catalog/12540/

Noilhan, J. and S. Planton, 1989: A simple parameterization of land surface processes for meteorological models. *Mon. Wea. Rev.*, 117, 536-549.

Stratman, D.R. and K.A. Brewster, 2014, Comparison of 24 May 2011 genesis and evolution of simulated mesocyclones using various microphysics schemes with 1-km resolution. 27th Conf. Severe Local Storms, Amer. Meteor. Soc., Paper 54.

Stratman, D.R. and K.A. Brewster, 2015: Verification of 24 May 2011 simulated mesocyclones using various microphysics schemes at 1-km grid resolution. 27th Conf. on Wea. Analysis and Forecasting & 23rd Conf. on NWP, Chicago, IL, Amer. Meteor. Soc., Paper 13A.6.

Sun, W.-Y., and C.-Z. Chang, 1986: Diffusion model for a convective layer. Part I: numerical 864 simulation of convective boundary layer. *J. Climate App. Meteorol.*, 25, 1445–1453.

Xue, M., K. K. Droegemeier, V. Wong, A. Shapiro, K. Brewster, F. Carr, D. Weber, Y. Liu, and D.-H. Wang, 2001: The Advanced Regional Prediction System (ARPS) - A multiscale nonhydrostatic atmospheric simulation and prediction tool. Part II: Model physics and applications. *Meteor. Atmos. Physics,* **76**, 143-165.

Xue, M., D.-H. Wang, J. Gao, K. Brewster, and K.K. Droegemeier, 2003: The Advanced Regional Prediction System (ARPS) – storm-scale numerical weather prediction and data assimilation. *Meteor. Atmos. Physics*, **82**, 139-170.

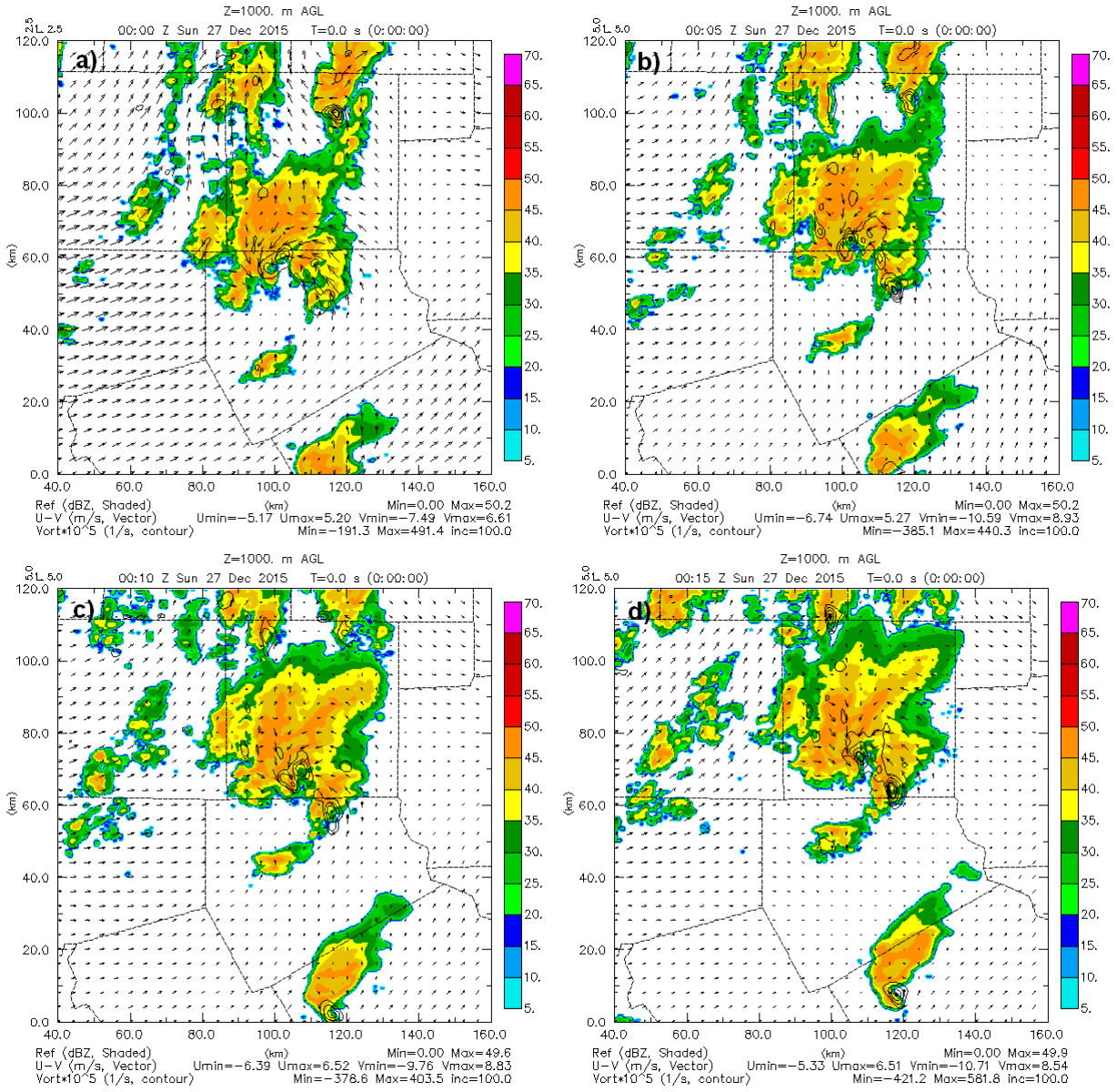

Figure 10. Real-time 400-m grid analyses for the 26 Dec 2015 Ovilla tornado. 1 km AGL horizontal cross-sections. Reflectivity (color), perturbation winds (m s^{-1}) and vertical vorticity (s^{-1} x 10^{-5}). All times UTC on 27-Dec-2015: a) 00:00, b) 00:05, c) 00:10, d) 00:15.

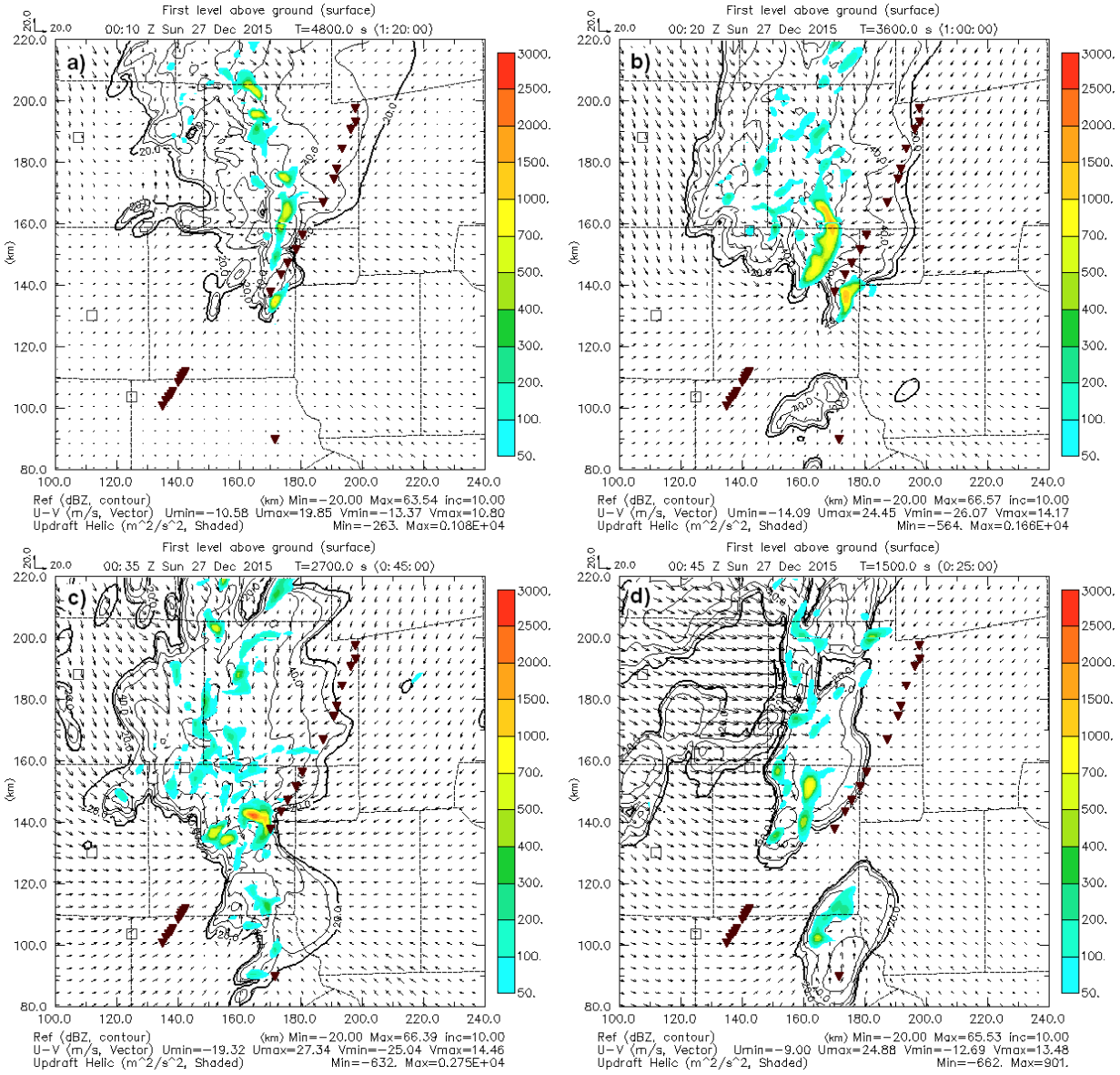

Figure 11. Four sequential real-time 1-km grid forecasts showing nearest forecast to the beginning of the 26 Dec 2015 Garland-Rowlett tornado track. Near surface perturbation winds and reflectivity (contours 1-6 km integrated updraft helicity (color shading, m^2 s^{-2}). Forecast initialized a) 2300 UTC, b) 2330 UTC, c) 0000 UTC, d) 0030 UTC.

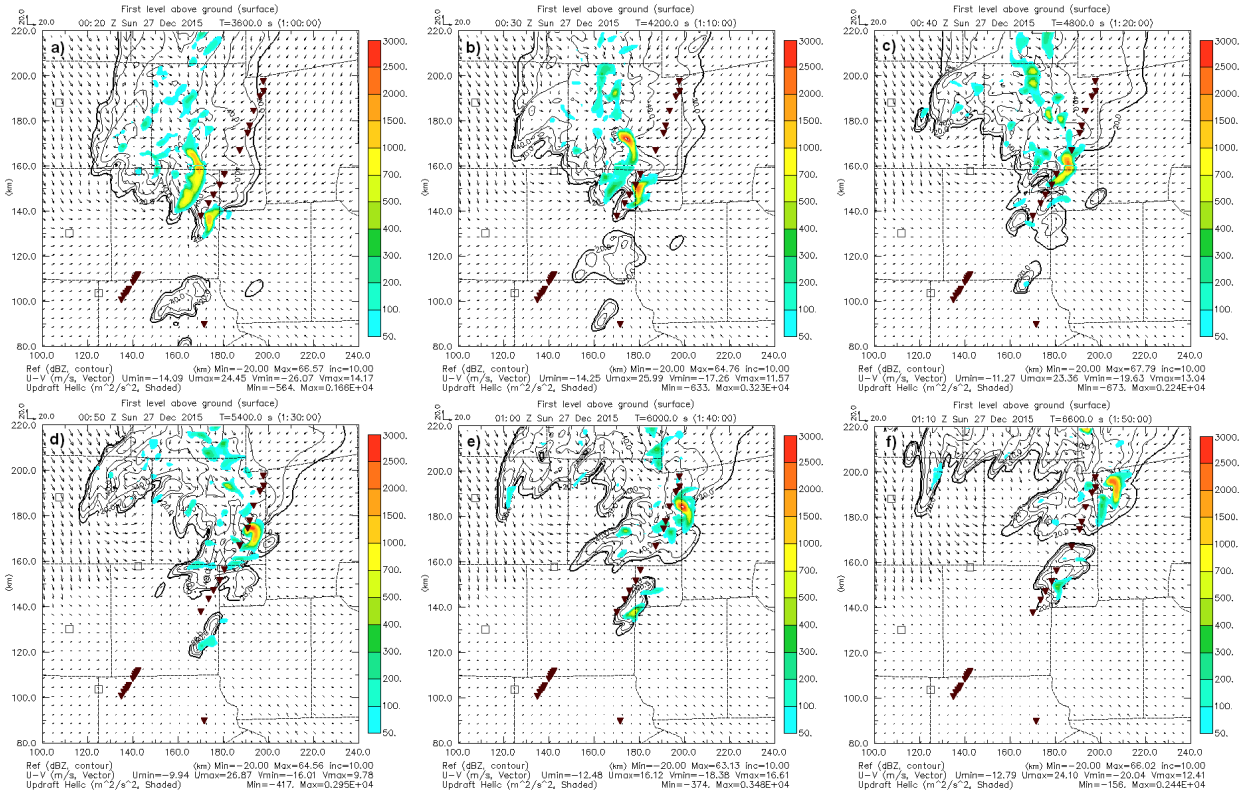

Figure 12. Real-time 1-km grid forecast output initialized at 2330 UTC 26 Dec 2015 for the Garland-Rowlett tornado. Near surface perturbation winds and reflectivity (contours), 1-6 km integrated updraft helicity (color shading, $m^2 s^{-2}$). Valid times UTC on 27-Dec-2015: a) 00:20, b) 00:30, c) 00:40, d) 00:50, e) 01:00, f) 01:10.